Published in final edited form as:
Magn Reson Med. 2008 November ; 60(5): 1037–1046. doi:10.1002/mrm.21682.

Non-Invasive Mapping of Human Trigeminal Brainstem Pathways

Jaymin Upadhyay[1], **Jamie Knudsen**[1], **Julie Anderson**[1], **Lino Becerra**[1], and **David Borsook**[1,2]

[1]P.A.I.N. Group, Brain Imaging Center, McLean Hospital, 115 Mill Street, Belmont, MA 02478, USA

[2]Athinoula A. Martinos Center for Biomedical Imaging Massachusetts General Hospital Harvard Medical School, Charlestown, MA 02129, USA

Abstract

The human trigeminal system mediates facial pain and somatosensory processing. The anatomic location of neuronal substrates and axonal pathways of the trigeminal system have previously been characterized with conventional *in vitro* methods. The present investigation implemented diffusion tensor imaging (DTI) and probabilistic tractography to first segment the peripheral trigeminal circuitry; trigeminal nerve branches (ophthalmic, maxillary and mandibular nerves), ganglion and nerve root. Subsequent segmentations involved the spinal trigeminal and trigeminal thalamic tracts, which respectively convey information to spinal trigeminal nuclei and ventral thalamic regions. This latter procedure also identified (1) spinal thalamic (anterolateral) system pathways (propagating pain and temperature information from the body); (2) trigeminal lemniscus (touch and face position) and 3) medial lemniscus (touch and limb position). The anatomic location of the identified pain and somatosensory pathways compared well with previous functional findings in human trigeminal system as well as the tract position in human histological cross-sections. Probabilistic tractography may be a useful method to further comprehend the functional and structural properties of trigeminal and other related systems. Application of DTI to map pain and somatosensory pathways in conjunction with a characterization of function properties of pain and somatosensory processing would further define the systematic changes that occur in trigeminal pathology.

Keywords

Diffusion Tensor Imaging; Trigeminal Nerve; Trigeminal Ganglion; Brainstem

Introduction

The trigeminal sensory system consists of (1) Trigeminal nerves (ophthalmic (V1), maxillary (V2) and mandibular (V3); (2) Trigeminal ganglion (TG); (3) Trigeminal nerve root (TNR); and (4) Central brainstem components, the spinal trigeminal nucleus (STN), spinal trigeminal tract (STr) and trigeminal thalamic tract (TTh) (1) (Figure 1). The peripheral components are made up of both motor and sensory branches. Motor branches are found in the mandibular nerve and originate in the motor nucleus of the STN. Sensory information including touch and position is conveyed by sensory afferents to the principal

Address correspondence to: Jaymin Upadhyay, Ph.D, P.A.I.N. Group, Brain Imaging Center, McLean Hospital, Harvard Medical School, 115 Mill Street, Belmont, MA 02478, USA, Tel: +1-617-855-2714 / Fax: +1-617-855-3772, Email: jayminu@mclean.harvard.edu.

sensory nucleus (Pr5), while pain and temperature fibers terminate in trigeminal nuclei, caudalis, interpolaris and oralis. The TNR enters the brainstem at the mid-pons and travels in rostral and caudal directions to various STN components. The central projections for pain and temperature sensation from the STN send afferents in the dorsal TTh that joins the spinal thalamic (STh) tract (anterolateral (AL) system) (Figure 1). Similarly, the trigeminal lemniscus (also referred to as ventral TTh) and medial lemniscus convey both touch and position information from the face and body, respectively. These parallel tracts run in very close proximity between pontine and thalamic regions.

The trigeminal system has features that make it a unique system to study functional connectivity of somatosensory pathways in the brainstem from peripheral inputs, intrabrainstem connections and central projections from the STN. For example, in the trigeminal system, there is a clear distinction of the three trigeminal nerves, as well as the somatotopic and functional segregation present throughout the brainstem and cortex (2,3). Previously, functional magnetic resonance imaging (fMRI) has been used to evaluate activations in the TG and STN to mechanical and thermal stimuli (2-5). While we and others have begun to use functional and structural observations to investigate changes in the human trigeminal system in clinical populations, the lack of a specific and objective method for defining the structural connectivity of the trigeminal system has been lacking (6-9).

The neuronal substrates and axonal pathways that form the human trigeminal system have in large part been anatomically characterized by postmortem histological techniques or contrast-enhanced MRI (10-15). What these methods and observations from these studies cannot easily facilitate is a more direct link between functional properties of trigeminal neuronal structures defined by functional imaging with microstructural properties of the axonal pathways that connect them, and to do so in a non-invasive manner. Such an approach where structural connectivity could more easily be related to function would allow for a better understanding of the neurobiology of healthy and diseased states (e.g. trigeminal neuropathy) of trigeminal and AL systems; from periphery to cortex.

Here we use diffusion tensor imaging (DTI) and probabilistic tractography to segment the human trigeminal circuitry based on the known pathways of the system (16-18). Specifically we wished to define (1) the peripheral trigeminal components (three trigeminal divisions, TG and TNR); (2) projections of the TNR into the brainstem; and (3) fiber projections within the brainstem and to the thalamus. Our results indicated that this anatomic technique can be implemented to map the known pain and somatosensory pathways in healthy subjects, and potentially in diseased states where the peripheral and central pathways are likely altered.

Materials and Methods

Subjects

Eight healthy subjects were scanned for this study (6 males and 2 females; age range (32.2 ± 12.8)). All subjects gave informed consent prior to the scanning session. This study was approved by the McLean Hospital Institutional Review Board.

Data Acquisition

All data were collected on a 3 Tesla Siemens Trio scanner with an 8-channel phased array head coil (Erlangen, Germany). DTI data were collected using a single shot-twice refocused echo planar pulse sequence at a $1.75 \times 1.75 \times 2.5$ mm^3 resolution. A single non-diffusion weighted ($b = 0$ sec/mm^2) volume was collected, while 72 distinct diffusion-weighted volumes were collected at $b = 1000$ sec/mm^2 (TR = 7900 msec, TE = 92 msec, 5/8 partial Fourier, 3-fold SENSE acceleration). Fifty axial slices were sufficient to cover the entire

cerebral cortex and cerebellum. Total acquisition time for DTI datasets was ~11 minutes. For each subject, the SNR was measured in non-diffusion weighted images in brainstem. The mean (n=8) ± standard deviation was measured to be 4.82 ± 1.85. T_1-weighted structural images were acquired using a 3-D magnetization-prepared rapid gradient echo (MPRAGE) sequence at a resolution of 1.0 × 1.0 × 1.0 mm^3 (TR = 2100 msec, TE = 2.74 msec, TI = 1100 msec, Flip angle = 12°, 128 sagittal slices) (19).

Data Analysis

Single subject data analysis was performed using FMRIB Software Library (FSL) (www.fmrib.ax.ac.uk/fsl). DTI datasets were initially corrected for eddy current distortion and head motion corrected using an affine registration (20,21). For this particular correction the non-diffusion weighted volume was used as the reference volume. To co-register the DTI and MPRAGE datasets it was first necessary to skull strip the non-diffusion weighted and MPRAGE volumes (22). Once an automated affine registration was performed to the skull stripped datasets additional manual registration was carried out for each subject (20,21). The latter was performed by manipulation of each subject specific transformation matrix outputted by the affine registration procedure.

Probabilistic diffusion tensor tractography was performed using the modeling technique proposed by Behrens and colleagues (17,18,23). In this modeling technique, the probability density functions (PDFs) of each voxel or the local model of diffusion in the DTI volume are first defined using a Markov Chain Monte Carlo sampling method. By implementing the Markov Chain Monte Carlo method, a distribution of fiber orientations or principal diffusion direction within each DTI voxel are modeled and in turn, are used to estimate the measured diffusion MR signal. The PDFs for each voxel give an account of uncertainty of the modeling parameters used to describe the measured diffusion-weighted MR signal. Thus, if it is determined that more than one principal diffusion direction can better estimate the measured diffusion MR signal; it is likely that multiple fiber orientations or a case of crossing fibers is present with a particular voxel. Once the local or voxel based PDFs are defined, a global or whole DTI volume PDF can be calculated to describe the uncertainty or confidence of connectivity between specific regions of interest (ROIs), be it a single point or entire neuronal substrate, and the rest of the DTI volume. Using the previously generated local PDFs, a probabilistic rather than deterministic streamline approach is taken. In the probabilistic streamline method: (1) A connection pathway is begun at a specified starting ROI; (2) A selection of random sample of fiber distribution are made within voxels that are at the newest ‘edge’ of the pathway; (3) A continuous forward progression of the tracting is carried out at a specified incremental distance along the selected fiber distribution; and (4) Probabilistic streamline tracting is terminated once a stopping criterion for tract tracing is present (23). This is in contrast to earlier deterministic streamline tractography algorithms where progression of a fiber pathway is determined by changes in curvature or principal diffusion directions occurring above a specified threshold and also presence of diffusion anisotropy within a voxel that is below a specified threshold. This causes probabilistic diffusion tractography to be less limited in regions where low diffusion anisotropy exists.

Lastly, to better account for the presence of more than one fiber orientation within a voxel and more accurately characterize a fiber pathway, the forward progression of probabilistic streamline is not necessarily based on which fiber distribution corresponds to the principal diffusion direction, but rather which distribution of fiber orientations best matches the fiber orientation from the previous step (17). By repeating the streamline probabilistic procedure numerous times (5000 iterations were performed in this study), it is possible to obtain the global PDF pertaining to the connectivity between two or more ROIs. The probability of a specific voxel being part of a pathway is determined by simply dividing the number of probabilistic streamlines going through a voxel by the total number of probabilistic

streamlines generated during the entire simulation. To threshold probabilistic tractography maps, the minimum probability threshold was set to at least 2% of the maximum probability.

Seeding Masks

Segmentation 1—For each subject a seeding mask demarcating the section of the trigeminal nerve root (TNR) lying between the trigeminal ganglion (TG) and pons was made on axial slices of the coregistered MPRAGE volume (Figure 2A). Performing probabilistic tractography using the TNR seeding mask not only identified the TG, but also the TNR as it traversed the pons, spinal trigeminal (STr) tract, anterolateral (AL) tracts, dorsal trigeminal thalamic (dTTh) tract and segments of the medial lemniscus (ML) and tegmental tract (TT) (Figure 4). Tracts of the trigeminal system, AL system, ML, etc are adjacent brainstem pathways running in parallel. The AL tracts include the spinal thalamic (STh), spinal mesencephalic (SM) and spinal reticular (SR) tracts. However, with regards to the AL tracts, the SR tract does not project to the midbrain region as do STh and SM tracts. The above mentioned tracts depicted in Figure 4 did not pass statistical threshold across all eight subjects.

Segmentation 2—By knowing the position of tracts such as the STr and AL within the brainstem in conjunction with a general knowledge of the spinal trigeminal nucleus (STN) and principal sensory nucleus (Pr5), it was possible to first segment the projection of the TNR into the pons to the point of termination in the Pr5 and STN. The TNR projections into the dorsal regions of the pons were obtained by using the TNR seeding mask prior to entry into the pons and also, waypoints that contained the STr and AL at the level of the mid-pons in ~2 MPRAGE axial slices (Figure 5). The STr and AL waypoints were slightly extended ~1-2 mm to include adjacent nuclei (i.e. STN and Pr5).

Segmentation 3—To segment the descending pathways (STr), and ascending pathways (AL, trigeminal lemniscus (TL) and medial lemniscus (ML)), seeding masks (white asterisks) were created in lateral region of the medulla and waypoints in the midbrain, where descending and ascending pathways were initially observed (Figure 6). The masks shown in Figures 5 and 6 were then used during waypoint probabilistic tractography between two ROIs to more accurately characterize the TNR as it projects into the pons as well as other brainstem pathways mentioned.

Segmentation 4—To segment the trigeminal (STr, dTTh and TL), AL and ML system pathways as they ascend to the thalamus, (collectively referred to as the ascending sensory system pathways (ASP)), two seeding masks were placed in the left and right halves of the pons in regions of the trigeminal, AL, and ML tracts (Figure 7). In each half of the pons one seeding mask was slightly medial to the other seeding masks, but was still in close proximity to the previously identified tracts. Two seeding masks were used in each halve in order to decipher if a more medial or more lateral seeding masks consistently identifies particular trigeminal, AL or ML system pathways. More than two seeding masks would likely increase the chances of identifying pathways not associated with trigeminal, AL or ML systems. Separate seeding masks in left and right halves of the pons were used to determine if pathways correctly remain in a single hemisphere as the pathway projects superiorly between pontine and thalamic pathways or if there is erroneous crossing over of the two pathways. In this last procedure, all possible pathways projecting through the seeding masks were considered and waypoints were not used as constraints.

Results

The results are presented in three sections (1) peripheral nerve; (2) trigeminal tracts and (3) brainstem projections.

DTI of the Peripheral Nerve Branches, Ganglion and Trigeminal nerve

The three peripheral branches, V1, V2 and V3, of the trigeminal system are shown in Figures 2 and 3. Figure 2A shows both an atlas based representation (top) as well as the gross anatomy (middle) of the TG, TNR and peripheral trigeminal nerve branches (24,25). DTI-based mapping (bottom) of the peripheral trigeminal anatomy yielded a very similar pattern when compared with the known anatomy. The TNR seeding mask (blue asterisk) identified the TG and the division of V1, V2 and V3 within the TG in the sagittal plane. Those regions of the TG and peripheral branches demarcated in yellow have the highest probability value, while those demarcated in blue have a lower probability value. This color attribution is true in all subsequent images and results (Figures 3, 5 and 6). Performing probabilistic tractography using the TNR seeding mask enabled the three division of the trigeminal nerve to be identified in 7 out of 8 subjects. (Data for the subject where trigeminal nerve divisions were not identified are shown in Figure 7). The inability to identify the peripheral branches in Subject 8, and also, the full lengths of V1, V2 and V3, was caused by the enhanced signal loss and susceptibility artifact (i.e., image distortion). The inability to measure more of the peripheral branches is a limitation based on air- soft tissue and/or bone- soft tissue interfaces present in this region of the brain producing this susceptibility artifact.

Based on the above result, and given the defined location of the peripheral trigeminal branches inputs into the ganglion (Figure 2A and Figure 3), seeding masks were placed in the ‘termination’ points of V1, V2 and V3 (white asterisk in Figure 2C). This latter procedure gave a more specific segmentation of V1, V2 and V3. The results indicate how the three branches have very distinct anatomical positions within the TG, prior to forming the TNR. In addition, the present DTI results show the anatomical correlation with past functional imaging results of somatotopic activation (bottom of Figure 2C) within the ganglia in a prior report of healthy humans were subjected to painful and mechanical stimuli in distinct facial regions; specifically where V1, V2 and V3 trajectories innervate (2). To further depict V1, V2 and V3 projections, coronal cross sections through the TNR and TG are given (Figure 2B). Coronal slice Y=127 shows that V1, V2 and V3 cannot be differentiated within the TNR; however an anterior progression towards the TG shows a clear distinction of the three branches. DTI-based characterization of peripheral trigeminal anatomy is shown for three other subjects in Figure 3. Similar to the sagittal slice shown in Figure 2A, the results for each subject in Figure 3 were obtained by seeding the TNR and performing probabilistic tractography. Each sagittal cross section for each subject corresponds to the plane in which the three branches could be viewed.

Peripheral Projections to the Brainstem

Seeding the TNR identified other trigeminal system structures and pathways, and also, other brainstem pathways associated with pain and somatosensory processing (Figure 4). These pathways include the STr tract; the pathway was noted to have projection patterns similar to what is depicted in the atlas based image shown on the left in Figure 4 (26). A caveat of the finding, shown in Figure 4, is that the brainstem pathways did not pass the statistical threshold and were not necessarily confined to the pathways of the trigeminal (STr, dTTh and TL), AL or ML systems (i.e. tegmental tract (TT)). Also, trigeminal, AL and ML brainstem pathways run adjacent to each other and also project superiorly as a single fiber bundle in some sections of the brainstem. This feature in conjunction with the resolution at

which DTI data were collected, did not always allow for a definite distinction between these pathways.

Based on the observations depicted in Figure 4, the next step was to segment the TNR as it enters the brainstem at the mid-pontine level and projects to the STN and Pr5 (Figure 5). The TNR projection within the pons shown in Figure 5 was identified using the seeding masks located in the TNR (X=49) and STN at the level of the pons (oralis) and Pr5 (X=54) and performing waypoint probabilistic tractography analysis. Recall, the seeding region in sagittal slice X=54 was defined to some extent based on the previous findings shown in Figure 5. In sagittal slice X=49, the TNR (depicted in a yellow-red-blue color scheme) is clearly seen as it projects into the TG. As the sagittal cross sections are projected medially, the TNR projects dorsally (posterior) towards the Pr5 and nucleus oralis. The pathways running through Pr5 and oralis seeding regions were also identified and are shown in blue (X=52 to X=54). Showing the results of the TNR projection as determined by waypoint analysis and the single seeding mask tractography result gave a frame of reference as to where the TNR projects to and if the projection is anatomically correct. Using the STN/Pr5 seeding mask resulted in the following tracts to be segmented; dTTH, AL and sections of the TT. In addition, both tractography procedures yielded projections to cerebellar lobules IV and V.

Brainstem Mapping and Central Projections

Figure 6 shows a segmentation of the STr, AL, TL and ML system pathways that project between the medulla and midbrain. The dTTh was not observed. To achieve this segmentation, seeding masks (white asterisks in Figure 6A) were positioned in the lateral regions of the medulla and midbrain and waypoint probabilistic tractography was performed. Coronal slices through the brainstem where the trigeminal (STr and TL), AL and ML pathways are present are shown in Figure 6A. Red lines in each coronal slice represent the location of the axial slices shown in the middle row (Figure 6B). In the bottom row (Figure 6C), histological cross sections of the brainstem correspond to the general location of the axial slices shown above. The following pathways were observed at various levels of the brainstem: (1) *Medulla* → STr and AL; (2) *Medulla-Pons* → STr and AL; (3) *Pons* → STr and AL; and (4) *Midbrain* → AL, TL and ML. Red circles indicate the location of the STr, AL, TL or ML system pathways in each cross section. The location of the above mentioned brainstem pathways as determined by DTI and probabilistic tractography are in good agreement with histological description of tract location of various brainstem pathways (www.msu.edu/~brains).

Lastly, the pain and somatosensory system trajectories between the brainstem and ventral regions of the thalamus were mapped (Figure 7). As noted above, two seeding mask were positioned in both halves of the pons in regions corresponding to the position of the pathways of interest. All four seeding masks are not shown in axial slice (Z=102) in order show the pathways more clearly. Probabilistic tractography was independently performed on each of the four seeding mask to determine if distinct pathways could be mapped depending on how medial or lateral the seeding mask was located within the pons and also, to observe if pathways cross between left and right halves of the brainstem. Using two seeding masks in either half of the pons did not yield significantly different pathways. The resulting pathways always corresponded to trigeminal, AL and ML system pathways, but never one and not the other. Pathways were observed to cross into to contralateral side; however, the trajectories largely remained ipsilateral between the pons and thalamus. In Figure 7, regions of the pons and midbrain demarcated in blue were obtained by using right side seeding mask, while red regions represent pathways originating from the left side seeding masks. The principal observation shown in Figure 7, is the differentiation of the various trigeminal, AL and ML pathways within the pons and convergence into a single fiber bundle of the two

systems' pathways between midbrain and thalamic levels (Z=115 to Z=131). In pons, the STr, AL and dTTh pathways can be differentiated from TL and ML system pathways. Furthermore, STr and dTTh pathways can be differentiated from AL system pathways. In axial cross section Z=115 to Z=131, the ascending sensory system pathways are enclosed within the dashed circle. The ASP include: (1) spinal thalamic (STh) and spinal mesencephalic (SM) tracts of the AL system; (2) dTTh; (3) TL; and (4) ML. Only the STh tract of the AL system projects to the thalamus. The DTI-based segmentation of pain and somatosensory pathways (shown in the left column) again correlates well with the location of these same pathways in histological cross-sections (shown in right column (27). Because the results shown in Figure 7 were obtained without an ROI (waypoint) constrained probabilistic mapping analysis, other fiber pathways not directly associated with pain and somatosensory processing were also identified. These latter pathways include sections of pontocerebellar tract (PCT) and oculomotor nerve (OMN).

Discussion

The use of clinical contrast-enhanced MRI techniques have previously allowed for the *in vivo* evaluation of the trigeminal nerve root (TNR) and trigeminal ganglion (TG) at a gross level (10-12,24). With regards to non-invasive MR methods, advanced DTI pulse sequences have been developed and applied in order to evaluate the TNR and other cranial nerves (28,29). However, a finer brainstem pathway segmentation of the trigeminal system and other related pain and somatosensory systems is not possible with contrast-enhanced MRI and has not been previously carried out in a systematic manner using DTI. In the present study, it was established that DTI and probabilistic tractography can be utilized to non-invasively identify and map: (1) Peripheral components of the trigeminal nerve (ophthalmic (V1), maxillary (V2) and mandibular (V3) nerves), the TG and the TNR; (2) Afferent inputs to the spinal trigeminal nucleus (STN) (spinal trigeminal (STr) tract); and (3) Central projections from the STN, which include the trigeminal thalamic (TTh) tract, anterolateral (AL) system pathways, and lastly, trigeminal (TL) and medial (ML) lemnisci. The anatomic locations of these DTI-based pathways are in agreement with what is observed in previous histological and functional imaging investigations (2,24) and multiple brain atlases (25-27). Additionally, the observed peripheral trigeminal pathways were linked to the known functional properties, as related to mechanical and thermal sensation.

Apart from a basic and non-invasive segmentation of pain and somatosensory pathways in healthy subjects, DTI and probabilistic mapping would be interesting to implement in a patient population; for example, in individuals suffering from trigeminal neuralgia. It is plausible that if intra- or extra-axonal changes are present in affected white matter pathways, these changes would be reflected and can be quantified with diffusion measures such as fractional anisotropy, radial diffusivity, mean diffusivity, etc. Furthermore, if functional properties of pain and somatosensory systems are also found to be altered in specific patient populations, the link between neuronal functional and white matter structural properties in these patients can be better explored.

Mapping the Trigeminal Nerve Branches, Ganglion and Nerve Root

In this study, trigeminal system circuitry beginning at the periphery was first segmented by performing diffusion tensor probabilistic tractography. Depending on the specific seeding mask location within the peripheral circuitry, either a general location of the trigeminal branches (V1, V2 and V3), TG and TNR (Figures 2A and 3) was identified, or a much finer segmentation of V1, V2 and V3 at the TG level was observed (Figures 2B and 2C). The latter result is particularly interesting, given previous fMRI findings (Figure 2B) where application of mechanical and painful heat stimuli to three distinct regions of the face, yielded a somatopically organized functional activation map in the TG (2). The three regions

where the two types of stimuli were applied corresponded to the facial locations where V1, V2 and V3 innervate.

A limitation of echo-planar DTI is its significant vulnerability to susceptibility artifact and signal loss in regions where air-tissue or bone-tissue interfaces exists, and therefore, not allowing V1, V2 and V3 trajectories to be identified much beyond these interfaces. This is less so the case in other MRI techniques used to identify peripheral trigeminal system structures such as contrast-enhanced T_2-weighted MRI (10-12,24). However, despite this particular limitation of DTI, the similarity of DTI-based segmentation of the peripheral trigeminal system anatomy to previous histological (Figure 2) and the above referenced contrast-enhanced MRI findings, points to the value of using molecular water diffusion as a means to characterize fibronal organization in the peripheral trigeminal circuitry. In addition, since the integrity of each branch is dependent on the neuronal bodies in the ganglion, the ability to evaluate changes in this region may be more significant when applied to peripheral nerve changes (e.g., neuropathy).

Mapping the Brainstem Trigeminal Tracts

As depicted in Figure 4, seeding the TNR prior to its entry into the pons identified pain and somatosensory pathways in brainstem. Although these brainstem projections were in the correct anatomical location, they did not surpass the statistical threshold set for probabilistic tractography results. Nonetheless, the mapping results in Figure 4, gave impetus to apply probabilistic tractography to segment pain and somatosensory brainstem pathways in a more specific manner (Figures 5, 6 and 7).

In Figure 5, the TNR trajectory into dorsal mid-pontine regions is depicted as well as the spinal projection going through the spinal trigeminal nucleus (STN)/primary sensory nucleus (Pr5) seeding mask. As noted in the results, the TNR was found to project to slightly lateral pontine regions containing the STN (nucleus oralis) and Pr5 (see, Figures 1 and 4). In addition to the TNR, a pathway between the STN and Pr5 seeding region and cerebellum was identified. Trigeminocerebellar pathways have been observed in rat, rabbit, cat and other species (30-32). Human functional imaging studies have also shown cerebellar activation during mechanical and thermal stimulation, and cerebellum association with processing acute and chronic pain in a clinical population (33,34). However, due to the sparse understanding of both functional properties and structural connectivity in human cerebellum, it is not possible to determine if the cerebellar projection in Figure 5 is indeed a trigeminocerebellar projection or a brainstem-cerebellum pathway unrelated to either pain or somatosensory processing. It is likely that a combined DTI and functional imaging investigation involving mechanical and noxious stimulation will facilitate trigeminocerebellar pathways to be characterized in a more accurate way.

Once the TNR enters the pons, sensory information is conveyed via large diameter fibers to Pr5 (touch and position) or via smaller diameter fibers to the three components of the STN (temperature, itch and pain). The STr tract mediates sensory information to oralis, interpolaris and caudalis nuclei and runs alongside the STN and AL pathways (spinal thalamic (STh), spinal mesencephalic (SM) and spinal reticular (SR) tracts). Similar to STr and dorsal TTh (dTTh) tracts, AL pathways carry sensory information relevant to temperature, pain and itch from the body to (1) Contralateral ventral thalamic regions (STh): (2) Tectum and periaqueductal gray matter in the midbrain (SM); and (3) Reticular formation in the pons and medulla (SR). Sensory information processed in the STN ascends to predominately ventral thalamic region by way of the contralateral dTTh, which also projects alongside the AL system pathways. In an analogous manner, the TL (Pr5→ventral thalamus) conveys touch and position information from the face and runs together with

much the larger ML (dorsal column nuclei→ventral thalamus) which propagates touch and limb position.

Mapping Pain and Somatosensory Brainstem-Thalamic Pathways

In Figures 6 and 7, the descending STr tract and ascending dTTh, AL, TL and ML pathways are shown in conjunction with corresponding histological cross sections. By comparing the DTI based segmentation of pain and somatosensory pathways, (Figure 6B and left column in Figure 7), with the histological cross-sections (Figure 6C (www.msu.edu/~brains) and right column in Figure 7 (27)), it can be observed that DTI-based and histologically-based segmentation methods yield similar anatomical locations for the pathways of interests. The T_1-weighted cross-sections obtained in this study match the location of the adapted histological cross-sections. In Figure 6, the STr, AL, TL and ML pathways were identified between medullary and pontine brainstem sections. However, once at the midbrain level, AL pathways (STh and SM), sections of the TL and ML pathways were observed. Rather than seeding just the lateral regions of the medulla and midbrain (Figure 6), implementing multiple seeds in the pons (Figure 7) enabled the ascending sensory system pathways (ASP) to be better characterized. For example, the AL and ML pathways as they ascend to ventral thalamic regions were seen and resembled the same pathways shown in the stained cross-sections. Performing a non-waypoint tractography analysis did identify the PCT and OMN which are not directly associated with pain and somatosensory processing. However, performing a waypoint analysis could possibly limit what pathways could be identified, or yield a partial segmentation of specific pathways.

Study Limitations

As mentioned above, the susceptibility artifact did not enable the full projection of peripheral trigeminal nerve branches to be mapped out, and in case of Subject 8, these peripheral branches were not identified at all. It is noted, however, that the segmentation of brainstem pathways was reproducible across subjects. Aside from the issue of susceptibility artifact or enhanced signal loss a number of study limitations are worth noting. First, was the inability to solely segment specific brainstem pathways (i.e. STr, ML, etc) or brainstem pathways confined to a particular system (e.g., trigeminal, AL, etc). This was a direct result of the minimum in-plane resolution at which DTI data could be collected with 1.75×1.75 mm^2 in conjunction with the fact that these relatively narrow tracts of interest are adjacent to each other. This limitation is in contrast to more common histological staining or tracer studies where differentiating between trigeminal or AL pathways would be possible. Second, the contralateral projections of brainstem trigeminal circuitry that is known to exist at various STN levels were not observed. As noted in the methods section, the implemented probabilistic tractography algorithm the forward progression of the probabilistic streamline is based on the distribution of fiber orientations that predominately matches the orientation from the previous step or voxel. Thus, the technique is likely to find ipsilateral projection given that the seeding regions were in the very lateral regions of brainstem sections where projections are oriented in the rostral-caudal directions. Third, in addition to acquiring DTI at a higher resolution, procedures such as acquiring cardiac-gated DTI data could possibly improve the quality of data given the pulsation effects present in brainstem and subcortical regions (35). However, cardiac-gated DTI would lead to longer data acquisition times. Other DTI procedures that may have a more profound effect on DTI data quality include implementing more sophisticated DTI acquisition pulse sequences that reduce susceptibility artifact and yield more accurate diffusion tensors (28,29).

Conclusions

The approach we have defined may be used to evaluate specific changes in patients with trigeminal pathology (e.g., neuropathic pain). Previous fMRI and DTI investigations have

independently shown localized functional and structural deficits within the trigeminal system in patient populations (6,8,36). These earlier observation suggest that there is the strong likelihood of functional alterations at the neuronal level occurring simultaneously with changes in white matter in trigeminal system diseases. Thus, a combined functional imaging and DTI investigation would further enable an understanding of the trigeminal and other related systems in healthy and pathologic states.

Acknowledgments

The authors would like to thank the MR technical staff at the Mclean Hospital Brain Imaging Center and Eric Moulton, Ph.D for helpful discussion during the preparation of this manuscript. This work was support by grants from NINDS (5R01NS042721 and 5R01NS56195) to DB.

References

1. Waite, P.; Ashwell, K. The Human Nervous Sytem. Paxinos, G.; Mai, J., editors. San Diego: Elsevier Academic Press; 2004.
2. Borsook D, DaSilva AF, Ploghaus A, Becerra L. Specific and somatotopic functional magnetic resonance imaging activation in the trigeminal ganglion by brush and noxious heat. J Neurosci. 2003; 23(21):7897–7903. [PubMed: 12944520]
3. DaSilva AF, Becerra L, Makris N, Strassman AM, Gonzalez RG, Geatrakis N, Borsook D. Somatotopic activation in the human trigeminal pain pathway. J Neurosci. 2002; 22(18):8183–8192. [PubMed: 12223572]
4. Borsook D, Burstein R, Becerra L. Functional imaging of the human trigeminal system: opportunities for new insights into pain processing in health and disease. J Neurobiol. 2004; 61(1): 107–125. [PubMed: 15362156]
5. Brooks JC, Zambreanu L, Godinez A, Craig AD, Tracey I. Somatotopic organisation of the human insula to painful heat studied with high resolution functional imaging. Neuroimage. 2005; 27(1): 201–209. [PubMed: 15921935]
6. Becerra L, Morris S, Bazes S, Gostic R, Sherman S, Gostic J, Pendse G, Moulton E, Scrivani S, Keith D, Chizh B, Borsook D. Trigeminal neuropathic pain alters responses in CNS circuits to mechanical (brush) and thermal (cold and heat) stimuli. J Neurosci. 2006; 26(42):10646–10657. [PubMed: 17050704]
7. Borsook D, Burstein R, Moulton E, Becerra L. Functional imaging of the trigeminal system: applications to migraine pathophysiology. Headache. 2006; 46(Suppl 1):S32–38. [PubMed: 16927962]
8. Herweh C, Kress B, Rasche D, Tronnier V, Tröger J, Sartor K, Stippich C. Loss of anisotropy in trigeminal neuralgia revealed by diffusion tensor imaging. Neurology. 2007; 68(10):776–778. [PubMed: 17339587]
9. Hadjipavlou G, Dunckley P, Behrens TE, Tracey I. Determining anatomical connectivities between cortical and brainstem pain processing regions in humans: a diffusion tensor imaging study in healthy controls. Pain. 2006; 123(1-2):169–178. [PubMed: 16616418]
10. Yousry I, Moriggl B, Schmid UD, Naidich TP, Yousry TA. Trigeminal ganglion and its divisions: detailed anatomic MR imaging with contrast-enhanced 3D constructive interference in the steady state sequences. AJNR Am J Neuroradiol. 2005; 26(5):1128–1135. [PubMed: 15891171]
11. Ziyal IM, Sekhar LN, Ozgen T, Soylemezoglu F, Alper M, Beser M. The trigeminal nerve and ganglion: an anatomical, histological, and radiological study addressing the transtrigeminal approach. Surg Neurol. 2004; 61(6):564–573. discussion 573-564. [PubMed: 15165800]
12. Chavez GD, De Salles AA, Solberg TD, Pedroso A, Espinoza D, Villablanca P. Three-dimensional fast imaging employing steady-state acquisition magnetic resonance imaging for stereotactic radiosurgery of trigeminal neuralgia. Neurosurgery. 2005; 56(3):E628. discussion E628. [PubMed: 15730595]
13. Downs MD, Damiano TR, Rubinstein D. Gasserian Ganglion: appearence on contrast-enhanced MRI. AJNR Am J Neuroradiol. 1996; 17:237–241. [PubMed: 8938292]

14. Paxinos, G.; Huang, XF. Atlas of the Human Brain Stem. San Diego: Academic Press; 1995.
15. Usunoff KG, Marani E, Schoen JH. The trigeminal system in man. Adv Anat Embryol Cell Biol. 1997; 136:I–X. 1–126. [PubMed: 9257459]
16. Basser PJ, Pierpaoli C. Microstructural and physiological features of tissues elucidated by quantitative-diffusion-tensor MRI. J Magn Reson B. 1996; 111(3):209–219. [PubMed: 8661285]
17. Behrens TE, Berg HJ, Jbabdi S, Rushworth MF, Woolrich MW. Probabilistic diffusion tractography with multiple fibre orientations: What can we gain? Neuroimage. 2007; 34(1):144–155. [PubMed: 17070705]
18. Behrens TE, Johansen-Berg H, Woolrich MW, Smith SM, Wheeler-Kingshott CA, Boulby PA, Barker GJ, Sillery EL, Sheehan K, Ciccarelli O, Thompson AJ, Brady JM, Matthews PM. Non-invasive mapping of connections between human thalamus and cortex using diffusion imaging. Nat Neurosci. 2003; 6(7):750–757. [PubMed: 12808459]
19. Mugler JP 3rd, Brookeman JR. Three-dimensional magnetization-prepared rapid gradient-echo imaging (3D MP RAGE). Magn Reson Med. 1990; 15(1):152–157. [PubMed: 2374495]
20. Jenkinson M, Bannister P, Brady M, Smith S. Improved optimization for the robust and accurate linear registration and motion correction of brain images. Neuroimage. 2002; 17(2):825–841. [PubMed: 12377157]
21. Jenkinson M, Smith S. A global optimisation method for robust affine registration of brain images. Med Image Anal. 2001; 5(2):143–156. [PubMed: 11516708]
22. Smith SM. Fast robust automated brain extraction. Hum Brain Mapp. 2002; 17:143–155. [PubMed: 12391568]
23. Behrens TE, Woolrich MW, Jenkinson M, Johansen-Berg H, Nunes RG, Clare S, Matthews PM, Brady JM, Smith SM. Characterization and propagation of uncertainty in diffusion-weighted MR imaging. Magn Reson Med. 2003; 50(5):1077–1088. [PubMed: 14587019]
24. Williams LS, Schmalfuss IM, Sistrom CL, Inoue T, Tanaka R, Seoane ER, Mancuso AA. MR imaging of the trigeminal ganglion, nerve, and the perineural vascular plexus: normal appearance and variants with correlation to cadaver specimens. AJNR Am J Neuroradiol. 2003; 24(7):1317–1323. [PubMed: 12917119]
25. Gray, H. Anatomy of the Human Body. Philadelphia: Lea & Febiger; 1918.
26. Nieuwenhuys, R.; Voogd, J.; van Huijzen, C. The Human Central Nervous System; A Synopsis and Atlas. New York: Springer-Verlag; 1981.
27. Martin, J. Neuroanatomy: Text and Atlas. New York: McGraw-Hill; 2003.
28. Koch M, Glauche V, Finsterbusch J, Nolte U, Frahm J, Weiller C, Büchel C. Distortion-free diffusion tensor imaging of cranial nerves and of inferior temporal and orbitofrontal white matter. Neuroimage. 2002; 17(1):497–506. [PubMed: 12482102]
29. Kabasawa H, Masutani Y, Aoki S, Abe O, Masumoto T, Hayashi N, O K. 3T PROPELLER diffusion tensor fiber tractography: a feasibility study for cranial nerve fiber tracking. Radiat Med. 2007; 25(9):462–466. [PubMed: 18026904]
30. Yatim N, Billig I, Compoint C, Buisseret P, Buisseret-Delmas C. Trigeminocerebellar and trigemino-olivary projections in rats. Neurosci Res. 1996; 25(3):267–283. [PubMed: 8856723]
31. Ikeda M, Matsushita M. Trigeminocerebellar projections to the posterior lobe in the cat, as studied by anterograde transport of wheat germ agglutinin-horseradish peroxidase. J Comp Neurol. 1992; 316(2):221–237. [PubMed: 1374086]
32. Bukowska D, Mierzejewska-Krzyzowska B, Zguczynski L. Topography and axonal collaterals of trigeminocerebellar projection to the paramedian lobule and uvula in the rabbit cerebellum. Acta Neurobiol Exp (Wars). 2006; 66(2):145–151. [PubMed: 16886725]
33. Maarrawi J, Peyron R, Mertens P, Costes N, Magnin M, Sindou M, Laurent B, Garcia-Larrea L. Motor cortex stimulation for pain control induces changes in the endogenous opioid system. Neurology. 2007; 69(9):827–834. [PubMed: 17724284]
34. Borsook D, Moulton EA, Tully S, Schmahmann JD, Becerra L. Human cerebellar responses to brush and heat stimuli in healthy and neuropathic pain subjects. Cerebellum. 2007:1–21.
35. Nunes RG, Jezzard P, Clare S. Investigations on the efficiency of cardiac-gated methods for the acquisition of diffusion-weighted images. J Magn Reson. 2005; 177(1):102–110. [PubMed: 16112886]

36. DaSilva AF, Granziera C, Tuch DS, Snyder J, Vincent M, Hadjikhani N. Interictal alterations of the trigeminal somatosensory pathway and periaqueductal gray matter in migraine. Neuroreport. 2007; 18(4):301–305. [PubMed: 17435592]

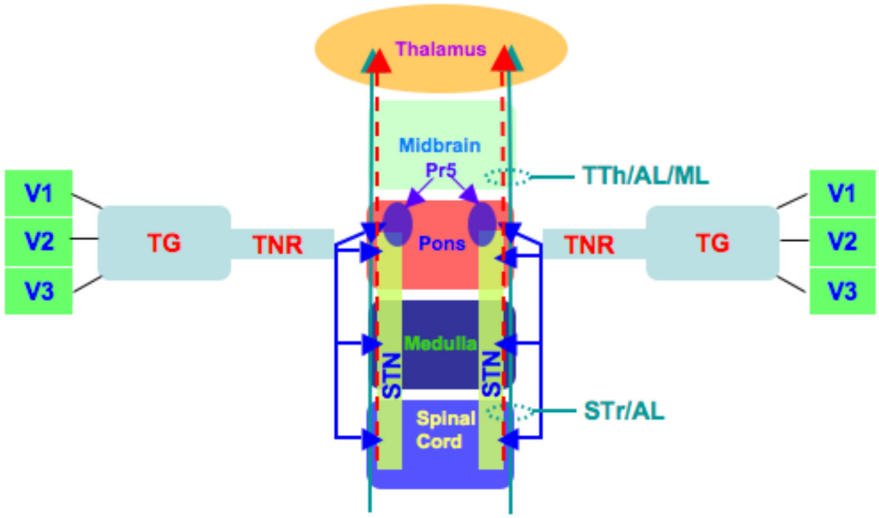

Figure 1. Pain and Somatosensory Pathways

A schematic is shown of pain and somatosensory neuronal substrates and the pathways that connect them. Beginning at the periphery, the three trigeminal branches, V1 (ophthalmic), V2 (maxillary) and V3 (mandibular), project to the trigeminal ganglion (TG) and converge to form the trigeminal nerve root (TNR). Upon entry into the brainstem at the pons, the TNR innervates all three spinal trigeminal nuclei (STN), caudalis, interpolaris and oralis, and the principal somatosensory nucleus (Pr5). Trigeminal (STr and TTh (dashed red arrow)), anterolateral (AL) and medial lemniscus (ML) (green arrow) system pathways traverse the brainstem in parallel between the spinal cord and thalamus. Ventral TTh (trigeminal lemniscus) and dorsal TTh tracts are jointly denoted as TTh. The AL pathways include spinal reticular, spinal mesencephalic and spinal thalamic tracts. With regards to trigeminal pathways, the STr projects up to Pr5 and oralis. Facial pain and somatosensory information is further propagated to the thalamus via the TTh tract. The ML runs in parallel and is adjacent to trigeminal and AL tracts between pontine and thalamic levels. Both ipsilateral and contralateral trigeminal and AL pathways exist in spinal cord, medulla and inferior pons. Contralateral projections are depicted in Figure 3.

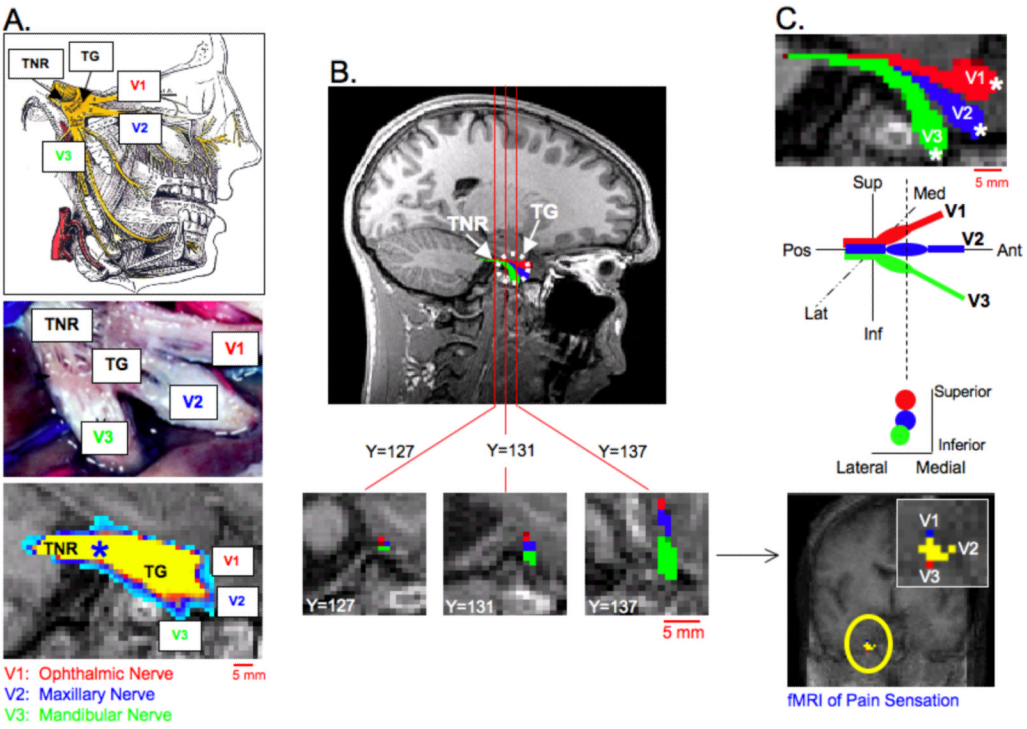

Figure 2. Peripheral Branches of Trigeminal System I

A. Anatomy of the Trigeminal Nerve Root (TNR), Trigeminal Ganglion (TG) and division of the peripheral trigeminal nerve branches. The three peripheral branches include V1 (ophthalmic nerve), V2 (maxillary nerve) and V3 (mandibular nerve). The top image in **A.** depicts the divisions of the trigeminal nerve at the level of the TG as well as the complete peripheral pathways of V1, V2 and V3 (25), while the middle image in **A.** was adopted from a histological investigation of the peripheral human trigeminal system by Williams et al. (24). The bottom image in **A.** was obtained by placing a seeding mask in the TNR (blue asterisk) and performing probabilistic tractography (Subject 1, See also *Segmentation 1* in **Methods and Materials**). All possible pathways through the seed regions were identified (waypoints not implemented). The TG was identified along with a division of three peripheral pathways within the TG. **B.** Using the initial tractography results shown in **A.** three seeding masks (white asterisks) were placed in the general regions of V1, V2 and V3 near the TG. Coronal slices are shown through the TNR and TG. A clear division of the three trigeminal nerve branches can be seen at the level of the TG (Y=137), but not in the TNR (Y=127). (Each coronal slice is of 1mm slice thickness and in native T_1-weighted anatomical space.) The latter probabilistic tractography results depicted a segmentation of the three trigeminal nerve branches, within the TG. **C**. An enlarged sagittal view of the three branches is shown in the top image. The differentiation of V1, V2 and V3 correlated well with previous functional imaging findings in the TG (2).

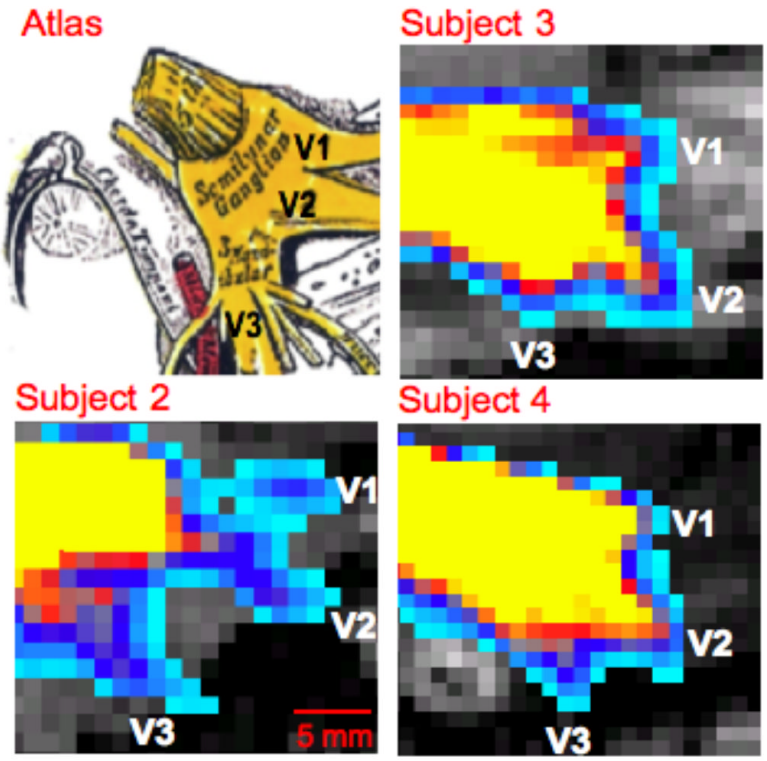

Figure 3. Peripheral Branches of Trigeminal System II

Trigeminal nerve branches at the level of the TG are shown in three other subjects (See also *Segmentation 1* in **Methods and Materials**). In each case the seeding masks for probabilistic tractography was placed in the TNR or TG. All possible pathways through the seed regions were identified (waypoints not implemented). An atlas based figure is shown in the upper left corner (25).

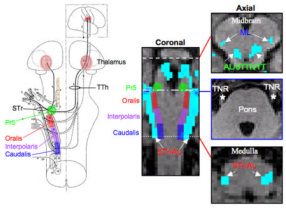

Figure 4. Brainstem Trigeminal System Pathways

Seeding masks within the TNR (white asterisks) not only identified the trigeminal ganglion and trigeminal nerve divisions, but also pathways in brainstem (Subject 7). All possible pathways through the seed regions were identified (waypoints not implemented; See also *Segmentation 1* in **Methods and Materials**). These pathways include the spinal trigeminal tract (STr), anterolateral system (AL) pathways, dorsal trigeminal thalamic (dTTh) tract, tegmental tract (TT) and medial lemniscus (ML). The AL pathways include the spinal thalamic, spinal mesencephalic and spinal reticular tracts. The probabilistic tractography procedure described in *Segmentation 1* identified pathways are in the correct anatomical location within the brainstem, but did not pass statistical threshold. The brainstem diagram on the left was adapted from Nieuwenhuys et al. (26).

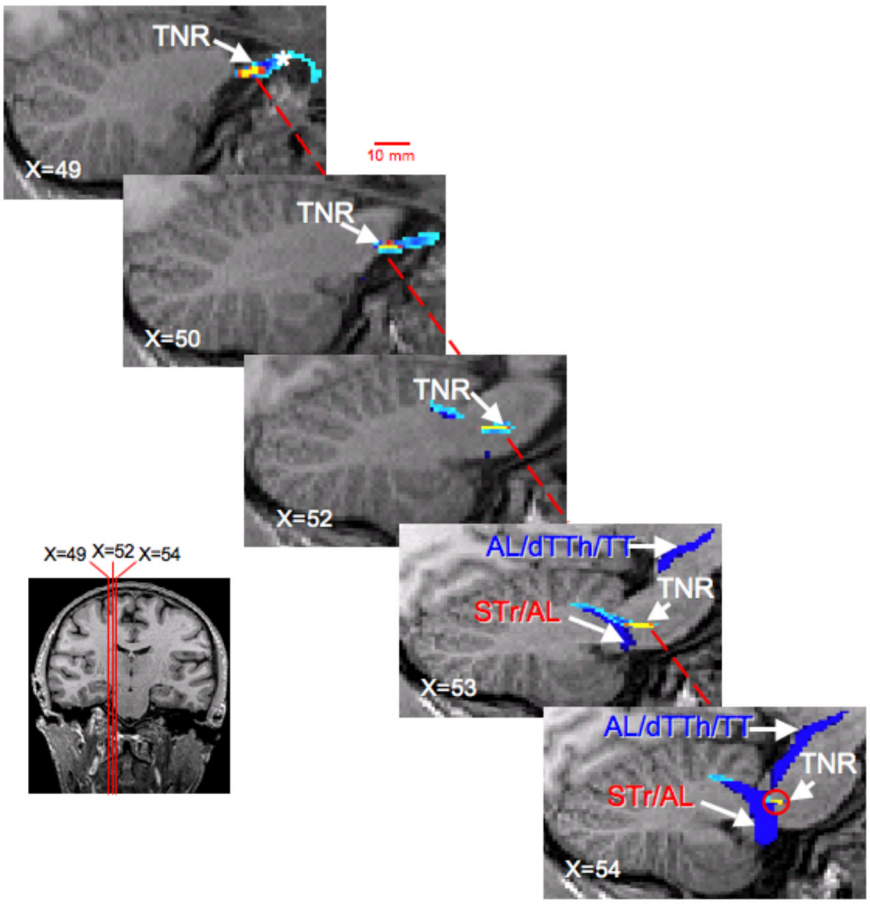

Figure 5. Trigeminal Nerve Root (TNR)

The projection of the TNR toward caudal pontine region is shown in six sagittal slices (Subject 1). To segment the TNR (shown in yellow and light blue), a seeding mask (white asterisks) was placed in the TNR, while waypoints were used in the spinal trigeminal tract (STr) at the level of the pons (See also *Segmentation 2* in **Methods and Materials**). In sagittal slices, X=52 to X=54, the pathway defined by using only the STr mask is shown. (Sagittal slices are consecutive 1mm slice thickness and in native T_1-weighted anatomical space.) The latter probabilistic tractography procedure segmented the spinal trigeminal tract (STr), spinal thalamic tract (STh), dorsal trigeminal thalamic (dTTh) tract and sections of the tegmental tract (TT).

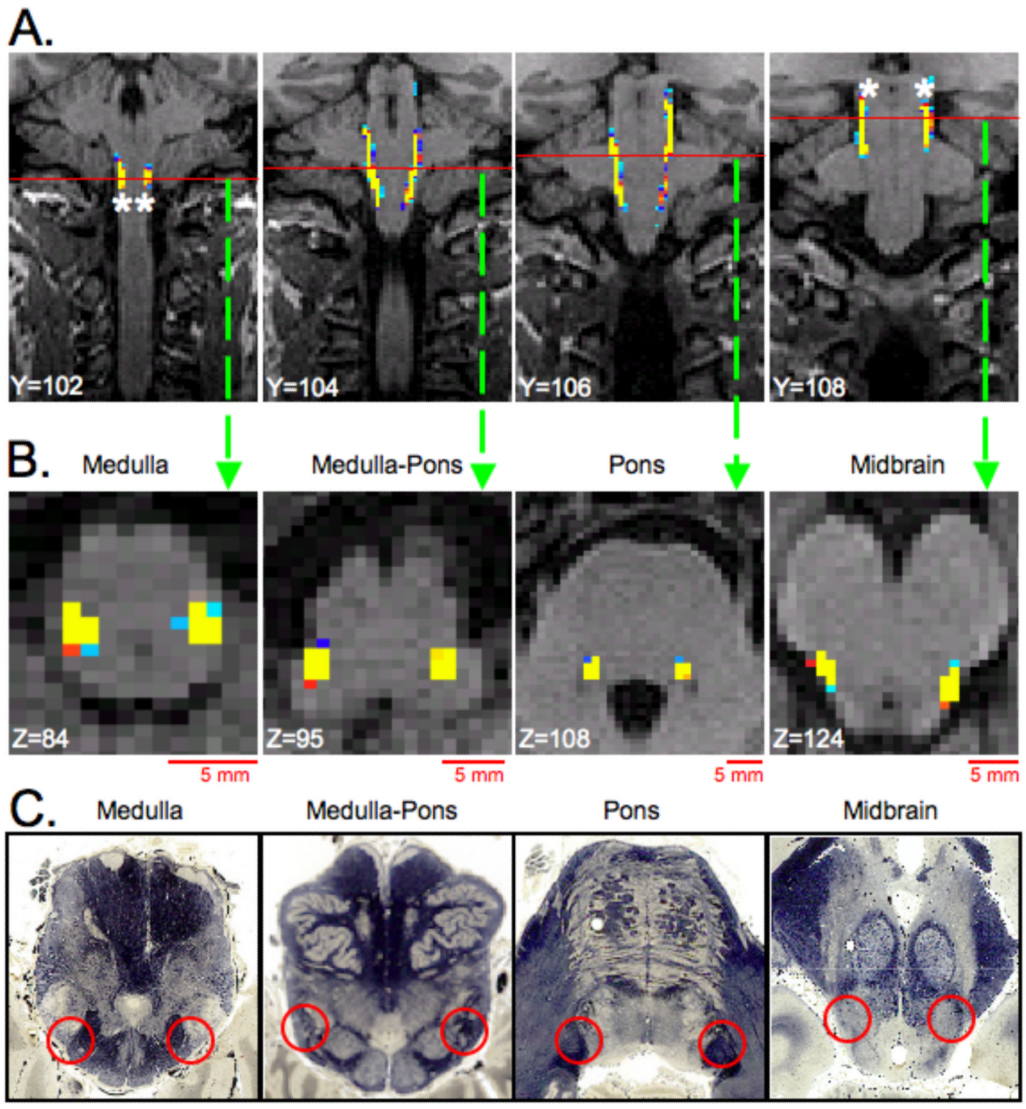

Figure 6. Trigeminal, Anterolateral, Trigeminal Lemniscus (TL) and Medial Lemniscus System Tracts

The spinal trigeminal (STr), anterolateral (AL), trigeminal lemniscus (TL) and medial lemniscus (ML) tracts were segmented by placing seeding masks (white asterisks) in lateral medulla regions and implementing waypoints (white asterisks) in lateral midbrain (Subject 6, See also *Segmentation 3* in **Methods and Materials**). The locations of the masks were based on results shown in Figure 3 and also a brainstem anatomical atlas (www.msu.edu/~brains). **A.** Coronal slices through the brainstem where the STr, AL, TL and ML tracts are present. Red lines in each coronal slice represent the location of the axial slices shown in **B. B.** Axial slices through 4 sections of the brainstem where STr, AL, TL and ML tracts are located. **C.** Histological cross sections of the brainstem corresponding to the general location of the axial slices shown in **B.** Red circles indicate location of the STr, AL, TL and ML in each cross section. (All coronal and axial slices have 1mm slice thickness and in native T_1-weighted anatomical space.) Histological cross sections were reprinted with permission from the Michigan State University Brain Biodiversity Bank (www.msu.edu/~brains) and the National Science Foundation.

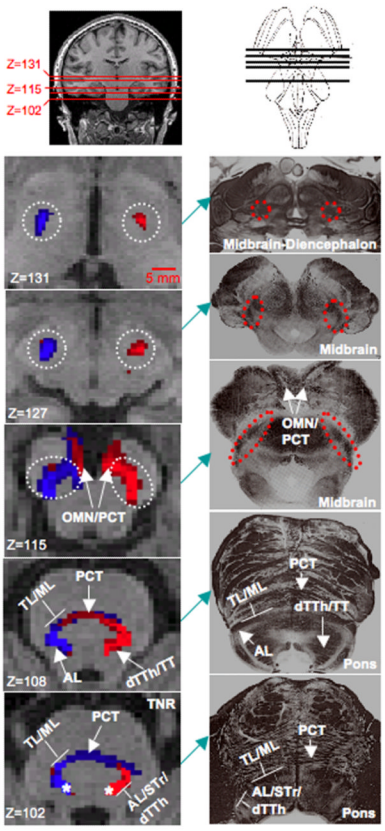

Figure 7. Ascending Sensory System Pathways

The ascending sensory system pathways consist of the anterolateral tracts (AL), dorsal trigeminal thalamic tract (dTTh), trigeminal lemniscus (TL) and medial lemniscus (ML). The spinal trigeminal tract (STr) were also identified in the pons. A DTI-based segmentation of these pathways is shown in the left column (Subject 8), while the corresponding histological cross-sections (adapted from Martin, 2003) of the brainstem are shown in the right column (27). Cross-sections in the right column are generally located in the same anatomical level as the cross section shown on the left. To segment these pathways two distinct seeding masks were placed in left and right halves half of the pons (white asterisks in Z=102), and all possible pathways through the seed regions were identified (waypoints not implemented). All four seeding mask are not shown (See also *Segmentation 4* in **Methods and Materials**). At the level of the pons (Z=102 and Z=108), the TL and ML are observed to run adjacent to each other and can be distinguished from STr, AL and dTTh tracts. The pontocerebellar tract (PCT) (Z=102 to Z=115) and oculomotor nerve (OMN) (Z=115) were also identified in the probabilistic tracting analysis. At the level of the midbrain (Z=115 to Z=127) the ascending sensory system pathway, white-dashed circle, project superiorly as a single bundle to ventral regions of the thalamus (Z=131). Between the midbrain and thalamus, the AL system no longer contains the spinal reticular tract. Red pathways originate from the left-hand seeding mask, while blue pathways originate from right-hand mask. Pathways were found to remain predominately ipsilateral between the pons and ventral thalamus. Axial slices are of 1mm slice thickness and in native T_1-weighted anatomical space.